Available online at www.sciencedirect.com

SCIENCE DIRECT

Biochimica et Biophysica Acta 1667 (2004) 26–37

BIOCHIMICA ET BIOPHYSICA ACTA
BBA

http://www.elsevier.com/locate/bba

Influence of the lipid composition on the kinetics of concerted insertion and folding of melittin in bilayers

Iren Constantinescu, Michel Lafleur*

Department of Chemistry, Université de Montréal, C.P. 6128, Succ. Centre Ville, Montréal, Québec, Canada, H3C 3J7

Received 21 April 2004; received in revised form 16 August 2004; accepted 30 August 2004
Available online 11 September 2004

Abstract

We have examined the kinetics of the adsorption of melittin, a secondary amphipathic peptide extracted from bee venom, on lipid membranes using three independent and complementary approaches. We probed (i) the change in the polarity of the ^{19}Trp of the peptide upon binding, (ii) the insertion of this residue in the apolar core of the membrane, measuring the ^{19}Trp-fluorescence quenching by bromine atoms attached on lipid acyl chains, and (iii) the folding of the peptide, by circular dichroism (CD). We report a tight coupling of the insertion of the peptide with its folding as an α-helix. For all the investigated membrane systems (cholesterol-containing, phosphoglycerol-containing, and pure phosphocholine bilayers), the decrease in the polarity of ^{19}Trp was found to be significantly faster than the increase in the helical content of melittin. Therefore, from a kinetics point of view, the formation of the α-helix is a consequence of the insertion of melittin. The rate of melittin folding was found to be influenced by the lipid composition of the bilayer and we propose that this was achieved by the modulation of the kinetics of insertion. The study reports a clear example of the coupling existing between protein penetration and folding, an interconnection that must be considered in the general scheme of membrane protein folding.

Keywords: Melittin; Lipid membrane; Kinetics; Fluorescence; Folding; Circular dichroism

The association of melittin, a 26-amino acid peptide extracted from bee venom [1,2], with lipid bilayers leads to considerable perturbations of membranes. At low concentration, melittin affects the permeability of lipid bilayers and leads to the release of the encapsulated materials. This phenomenon has been observed in the case of both model and biological membranes (e.g., Refs. [3–7]). The permeability perturbation induced by melittin has been shown to depend on the membrane lipid composition. It has been established that melittin-induced release from phosphatidylcholine vesicles was inhibited by cholesterol [7,8], and negatively charged lipids [6,8–12]. The origin of this inhibition was however different for these systems. The formation of a fluid but ordered phase in the presence of cholesterol [13–15] leads to a decrease of melittin affinity for bilayers and, consequently, reduces the leakage caused by the peptide [7,8,16]. On the other hand, the presence of negatively charged lipids in the membranes increases the membrane affinity of melittin, which is a cationic peptide, but anchors the peptide at the interface, preventing the relocation required to form leaks [6,9,17].

The association of melittin to lipid membranes has been investigated partly because this peptide has a secondary amphiphilic helix character [2,18–20] and is used as a model for this class of peptides. This motif is relatively common in biological systems. Several signal peptides that lead to the insertion of proteins in the specific membranes

Abbreviations: CD, circular dichroism; chol, cholesterol; POPC, 1-palmitoyl-2-oleoyl-*sn*-glycero-3-phosphocholine; POPG, 1-palmitoyl-2-oleoyl-*sn*-glycero-3-phosphoglycerol; 6,7Br$_2$PC, 1-(6,7-dibromo)palmitoyl-2-oleoyl-*sn*-glycero-3-phosphocholine; LUV, large unilamellar vesicles; PC, phosphocholine; Ri, incubation lipid/melittin molar ratio; SUV, small unilamellar vesicles; PS, phosphatidylserine; DMPC, dimyristoyl-*sn*-glycero-3-phosphocholine; DPPC, dipalmitoyl-*sn*-glycero-3-phosphocholine; DOPC, dioleoyl-*sn*-glycero-3-phosphocholine; DOPG, dioleoyl-*sn*-glycero-3-phosphoglycerol

* Corresponding author. Tel.: +1 514 343 5936; fax: +1 514 343 7586.
E-mail address: michel.lafleur@umontreal.ca (M. Lafleur).

0005-2736/$ - see front matter © 2004 Elsevier B.V. All rights reserved.
doi:10.1016/j.bbamem.2004.08.012

where they will accomplish their functions, also display a secondary amphiphilic helix structure [21,22]. Some proteins of the complement system, targeting foreign particles of the bloodstream and activating the cascade leading to their removal, also have segments that adopt secondary amphiphilic helix structure [23,24]. In addition, melittin has been a source of inspiration for the development of novel antiviral and antibacterial agents that act at the membrane level to cause leakage in their lethal mechanism [25–27]. In order to understand and develop these aspects, it is essential to get a detailed molecular description of melittin–lipid membrane interactions. In addition, this "simple" system is useful in establishing a physico-chemical basis describing membrane protein folding [28].

Few studies have examined the kinetics of melittin association with membranes. The kinetics of the formation of the defects leading to leakage has been found to be in the order of minutes [3,6,29,30]. The phenomena occurring with a shorter time scale have a particular interest. It was shown that melittin association with phosphatidylcholine membranes takes place in the order of milliseconds [31–34]. The kinetics of this phenomenon is still a matter of controversy as it is reported to be monophasic by some researchers [31,32], and biphasic by others [33,34]. The influence of the lipid composition on the kinetics of melittin–membrane association is still to be determined. The present work aims at gaining some understanding of the early events of melittin association with lipid membranes and how lipid composition influences the kinetics of these events.

We have characterized the first steps of the interaction of melittin with lipid membranes. The adsorption has been probed using three independent and complementary approaches. First, it is well established that the change of the polarity of the tryptophan environment can be observed by the hypsochromic shift of its fluorescence. Therefore, the transfer of ^{19}Trp of melittin from the aqueous milieu to membrane environment, which has a lower dielectric constant, can be probed by the changes in its fluorescence spectrum [35–37]. Second, we have probed the insertion of ^{19}Trp deeper in the bilayers by incorporating lipids bearing brominated acyl chains. Bromine atoms are good quenchers of Trp fluorescence, and the quenching occurs when the Br-Trp distance is in the order of 10 Å [38–40]. The Trp fluorescence quenching was therefore reporting the insertion of the ^{19}Trp in the apolar core of the lipid bilayers. Finally, circular dichroism (CD) was used to probe the folding of the peptide upon binding to lipid membranes. It is well established that free melittin monomer is essentially a random coil molecule, whereas it displays a high α-helix content when it is bound to membranes [18,41]. The combination of these three techniques, performed on the same systems, in the same conditions, provides a detailed picture of the first events of the peptide association. Three lipid compositions were investigated: 1-palmitoyl-2-oleoyl-*sn*-glycero-3-phosphocholine (POPC) bilayers, a zwitterionic membrane; POPC bilayers containing 1-palmitoyl-2-oleoyl-*sn*-glycero-3-phosphoglycerol (POPG), to examine the influence of negative charges; and POPC/cholesterol (chol) bilayers, a system forming a liquid ordered phase [14].

1. Materials and methods

Melittin was purified from bee venom (Sigma Co., St. Louis, MO) according to an established procedure [42]. Its purity was estimated to >96%, based on the analytical chromatogram recorded with a detection at 214 nm. POPC, and POPG were obtained from Northern Lipids Inc. (Vancouver, Canada), and 1-(6,7-dibromo)palmitoyl-2-oleoyl-*sn*-glycero-3-phosphocholine (6,7Br$_2$PC) was obtained from Avanti Polar Lipids (Alabaster, AL). Cholesterol and tryptophan were purchased from Sigma.

Lipid mixtures were obtained by mixing appropriate volumes of lipid stock solutions prepared by weight in benzene/methanol 95:5 (v/v). All the lipid proportions are expressed in mol. The organic solutions were freeze-dried for at least 18 h. The samples were hydrated with the buffer to provide a final lipid concentration between 10 and 20 mM, and, afterwards, were submitted to five freeze-and-thaw cycles, from liquid nitrogen to room temperature. The buffer was a 20 mM Hepes buffer containing 5 mM NaCl, 2 mM ethylenediaminetetraacetic acid (EDTA), at pH 7.4. The resulting multilamellar vesicles were extruded through polycarbonate filters with pore size of 50 nm in diameter (Nuclepore Whatman), using a Lipex extruder. The exact phospholipid concentration was determined using the Fiske–Subbarow assay [43]. The stock suspensions of large unilamellar vesicles (LUV) were diluted to provide a final lipid concentration of 3.15 mM. Melittin and tryptophan solutions were prepared in the same buffer and their concentrations were determined by their absorbance at 280 nm (the molar absorptivity coefficient at this wavelength is 5600 M^{-1} cm^{-1}) [44]. Aliquots of the melittin or tryptophan stock solutions were diluted to a final concentration of 35 μM.

1.1. Trp environment

The lipid suspension, and the melittin or Trp solution were introduced separately in two syringes. Appropriate volumes were injected in a 100-μl cell. For the Trp fluorescence, the excitation wavelength, and bandwidth were set at 280 and 4.6 nm, respectively. The equilibrium emission spectra were recorded 5 min after the mixing of the lipid suspension with melittin. One data point/2 nm was measured between 420 and 310 nm. In the kinetics mode, the fluorescence intensity was measured at 380 nm, for 2 s following the mixing of the lipid suspension and the melittin solution, with a sampling rate of 500 Hz. Between 25 and 75 acquisitions were co-added to improve the signal/noise ratio. The gain was adjusted to obtain a signal of 2.35 for

free melittin. The fluorescence intensity was corrected for the light scattering caused by the LUVs. In order to perform this correction, we recorded the fluorescence intensity of a tryptophan solution at the same concentration as the melittin concentration, in the presence and the absence of lipid LUVs. It has been shown that tryptophan practically does not interact with lipid membranes [45]. Therefore, the change in fluorescence intensity occurring in the presence of LUVs is due to the scattering of the exciting light or of the fluorescence. By ratioing the tryptophan fluorescence intensity obtained with and without LUVs, a correction factor was determined and melittin fluorescence intensities were multiplied by this factor. This factor was sensitive to the experimental conditions, including lipid composition of the LUVs and the lipid concentration, and was therefore determined for each system. For all the investigated systems, the value of this factor varied between 1.1 and 1.3.

1.2. Fluorescence quenching

The vesicles and melittin solutions were prepared as described above, except that the lipid composition included brominated lipids. 6,7Br_2-PC, and POPC were separately solubilized in a benzene/MeOH 95:5 (v/v) mixture. A phosphorus assay was performed on each solution to obtain the exact lipid concentration. Appropriate volumes of these phosphocholine (PC) solutions were mixed to obtain a molar proportion of 15% in brominated-PC. Subsequently, aliquots of these organic solutions were mixed with an organic solution of POPG or cholesterol to provide the desired mixtures. Control lipid mixtures, which did not include brominated PC, were prepared from the same organic solutions of individual lipids. The proportion of brominated PC is expressed relative to the total amount of PC (i.e. Br_2PC/[POPC+Br_2PC]). The proportions of cholesterol and POPG are expressed relative to all the lipids in the mixtures.

All the acquisition conditions were similar to those described above except that the bandwidth was set to 2.3 nm. The steady-state emission spectra were recorded between 450 and 300 nm with one data point/nm. Three scans were co-added. The kinetics measurements were performed over a 2-s period with a sampling rate of 500 Hz. The excitation wavelength was 280 nm and the emission wavelength was 351 nm for the PC systems, 350 nm for the PC/POPG systems, and 346 nm for the PC/cholesterol systems. These wavelengths were selected because they corresponded to an isoemissive wavelength for each system, as discussed in Results. Each kinetics trace is the average of 75–100 acquisitions, in order to improve the signal/noise ratio.

1.3. Circular dichroism

A melittin solution (35 μM) and lipid vesicles were prepared in Hepes buffer (5 mM, containing 10 mM NaCl, 2 mM EDTA, pH 7.4). Hepes concentration was reduced to 5 mM to minimize the buffer absorption. The experiments with POPC/POPG (97:3) mixtures, the system for which electrostatic interactions should have the most significant contribution, were also performed in 5 mM Hepes, 20 mM NaCl, 2 mM EDTA, in order to obtain an ionic strength similar to that used with the other sets of measurements. No significant differences were observed between the two sets of measurements, suggesting that this limited variation in ionic strength does not lead to measurable differences. Melittin solutions, lipid mixtures, and 50 nm vesicles were prepared according to the above description. A quartz cell with a 2 mm path length was used. The calibration of the CD spectrometer was performed using D-10-camphorsulfonic acid. Equilibrium CD spectra were recorded between 250 and 215 nm with an increment of 0.5 nm at 10 nm/min. Each spectrum is typically the average of 28 scans. For the kinetics measurements, the ellipticity at 222 nm was measured for 2 s with a sampling rate of 500 Hz. An average of 300–500 runs was obtained. All the traces were corrected (e.g. for the light scattering caused by the vesicles) by subtracting the signal of a blank containing everything but melittin. The helical fraction of the peptide was estimated from the average molar ellipticity per residue [θ] measured at 222 nm [46].

All the measurements were obtained at 25 °C on a Stopped-Flow SX.18 MV spectrometer (Applied Photophysics, Surrey, UK). This spectrometer allows both fluorescence and CD measurements, using the same stop-flow set-up. The dead time of the spectrometer has been determined to be less than 2 ms for the fluorescence measurements, and less than 5 ms for the CD.

2. Results

2.1. Trp environment

The kinetics of melittin association to lipid bilayers was followed by the variation of the melittin fluorescence intensity associated to its ^{19}Trp. In order to select the most appropriate wavelength for the kinetics measurements, steady-state fluorescence spectra of melittin–lipid systems were recorded. For example, Fig. 1 shows the fluorescence spectra of melittin free in solution, and bound to POPC membranes. The incubation lipid/melittin molar ratio (Ri) was 90 and, in these conditions, it is expected that all the melittin molecules are membrane-bound [7,37], and that the LUVs remain intact [7]. In the free form, the maximum of the melittin fluorescence at 354 nm, a value typical of water-exposed tryptophan, is in agreement with previous studies [35]. In agreement with previous reports [36], the maximum of the fluorescence intensity is shifted to 339 nm when melittin is bound to the POPC membranes; this shift indicates a less polar environment of the ^{19}Trp. For melittin binding to POPC/POPG mixtures, similar shifts were observed (data not shown). The emission maxima were at 338 and 337 nm for melittin bound to POPC/POPG 97:3

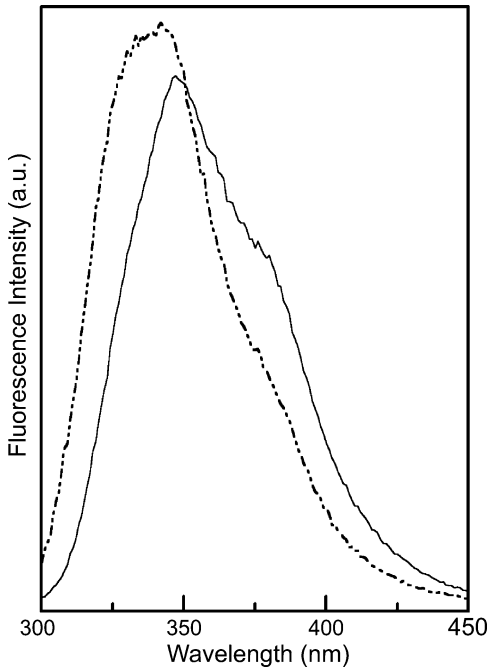

Fig. 1. Fluorescence spectra of melittin (—) free in solution, and (- - - -) bound to POPC bilayers (Ri=90; [POPC]=3 mM; [melittin]=35 μM). λ_{exc}=280 nm. The spectrum in the presence of LUVs was corrected as described in Materials and methods.

and 85:15, respectively. A more pronounced hypsochromic shift of the ^{19}Trp fluorescence of melittin in the presence of negatively charged lipids has already been reported [12,47]. In the case of POPC/chol system, for a Ri of 90, the shift of the ^{19}Trp fluorescence of melittin was less pronounced; the maximum was 347 nm (data not shown). According to previous work [7], melittin is not completely bound to the cholesterol-containing membranes in these conditions. This incomplete binding is the likely origin of the limited shift and this aspect is discussed below.

In order to probe the kinetics of the binding, we have recorded the variation of the fluorescence at 380 nm. This wavelength was selected because it corresponds to a wavelength where the intensity changes are the most pronounced. Moreover, at this position, the light scattering is less important and was easier to correct. First, we have examined the kinetics of the association of melittin to POPC membranes. The variations of fluorescence intensity as a function of time are represented in Fig. 2. The signal obtained from the dilution of free melittin with buffer is reproduced as a reference. The decrease in intensity occurred mainly during the first second. This decrease in intensity ($I(t)$) was simulated using a bi-exponential function:

$$I(t) = A_1\exp(-k_1t) + A_2\exp(-k_2t) + F$$

where k_1 and k_2 are the rate constants, A_1 and A_2, the pre-exponential factors, and F is the final fluorescence intensity. This type of decay is valid for two parallel events as well as for two irreversible sequential events [48]. The possible mechanisms associated to melittin association with the bilayers are discussed below. The fitted values are reproduced in Table 1. The sum of A_1, A_2, and F correspond reasonably well to the value obtained for free melittin. The trace could not be properly simulated by a mono-exponential.

Similar experiments were performed with LUV including negatively charged POPG. As for POPC system, the association kinetics of melittin to POPC/POPG LUVs can be fitted by a bi-exponential, and the parameters are reported in Table 1. Differences are observed compared to the values obtained with POPC. First, on the basis of the comparison between the fluorescence intensity obtained for free melittin and the sum of A_1, A_2, and F, it is found that a fraction of the fluorescence intensity variation happened during the dead time, and this fraction progressively increases as a function of the POPG content, going from 0 for pure POPC to 42% for POPC/POPG 85:15. Measurements were performed with LUVs containing 25% POPG but no change in fluorescence intensity were observed, the association being completed within the dead time of the set-up. Second, the rate constant k_1 increases with the POPG content, in agreement with a faster association of the toxin in the presence of POPG. The contribution of the first exponential, provided by A_1, is similar for LUVs containing up to 5% POPG. For the vesicles containing 15% POPG or more, the fittings seem to indicate a considerable decrease in

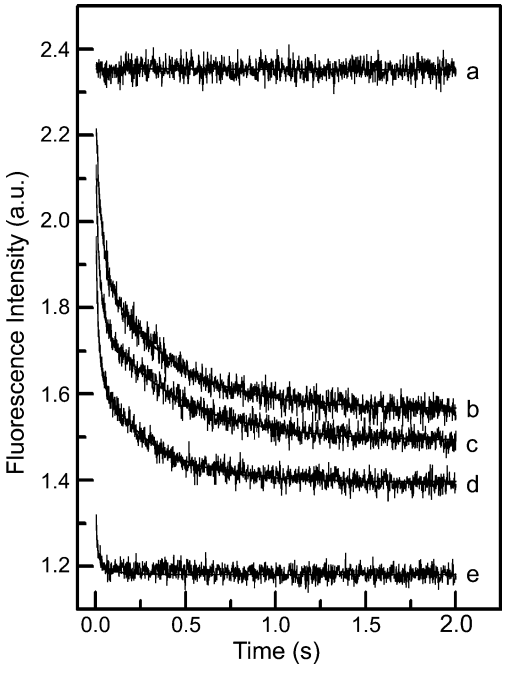

Fig. 2. Kinetics of melittin adsorption on POPC and POPC/POPG vesicles, as observed by the change of fluorescence intensity at 380 nm, as a function of time, λ_{exc}=280 nm. (a) Free melittin, (b) melittin with POPC, (c) melittin with POPC/POPG 97:3, (d) melittin with POPC/POPG 95/5, (e) melittin with POPC/POPG 85:15. (Ri=90; [phospholipid]=3 mM; [melittin]=35 μM). The curves were corrected for light diffusion caused by the presence of the lipid vesicles as described in Materials and methods.

Table 1
Parameters related to the change in polarity of ^{19}Trp during the association of melittin with lipid membranes

Parameters	POPC/melittin	(POPC/POPG) (97:3)/melittin	(POPC/POPG) (95:5)/melittin	(POPC/POPG) (85:15)/melittin	(POPC/chol) (70:30)/melittin	(POPC/chol) (70:30)/ melittin (Ri 129)
A_1[a]	0.33±0.01	0.33±0.01	0.32±0.01	0.11±0.01	0.23±0.01	0.25±0.01
k_1 (s^{-1})	32±2	48±3	69±4	77±9	40±3	45±3
A_2[a]	0.34±0.01	0.29±0.01	0.25±0.01	0.02±0.01	–	–
k_2 (s^{-1})	2.6±0.1	2.30±0.05	3.30±0.07	10±7	–	–
F[a]	1.57±0.01	1.49±0.01	1.40±0.01	1.18±0.01	2.06±0.01	1.960±0.001

The lipid composition is indicated at the top of each column and the Ri was 90 except where indicated.
[a] Volt.

A_1. However, it is likely an artefact associated with the kinetics of these systems that is too fast to be properly recorded. The contribution of the second exponential, represented by A_2, is decreased as a function of POPG to practically vanished when the POPG proportion reaches 15%. The more pronounced hypsochromic shift obtained in the presence of POPG, as discussed above, is also expressed by the decreasing F values. It is interesting to note that an amount as small as 3 mol% of POPG influences significantly the kinetics of the association of this cationic peptide. In order to be in conditions for which the signal variations can be properly recorded, we have examined the POPC/POPG 97:3 system with the other techniques.

The effect of cholesterol on the kinetics of melittin association to vesicles was also examined. In this case, a mono-exponential could be fitted (Fig. 3), and the resulting values are presented in Table 1. These experiments were performed for Ri of 90, and 129. The ratio of 90 is the lipid/melittin ratio used for the first set of experiments, whereas a ratio of 129 corresponds to the equivalent phospholipid/melittin ratio. No significant difference in the kinetics parameters was observed between these two data sets. The F value was slightly smaller in the latter case, likely associated to a larger proportion of bound melittin when more lipids were present. The extrapolated value for the initial fluorescence intensity (A_1+F) agrees well with the value measured for free melittin. By comparing the kinetics parameters obtained for bilayers in the presence and the absence of cholesterol, it seems that the association observed with POPC/chol LUV corresponds to the first component of the association of melittin to POPC LUVs.

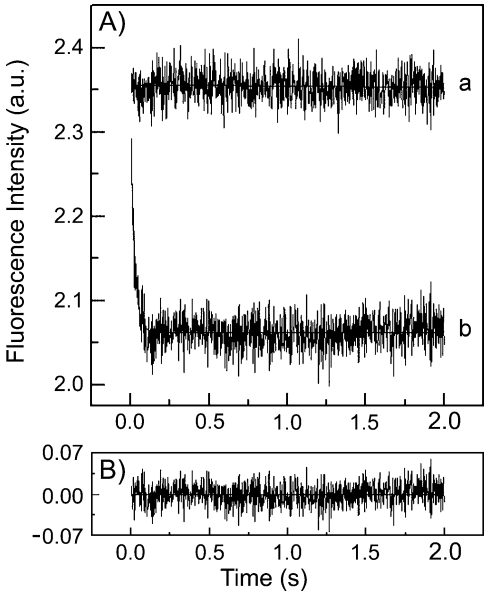

Fig. 3. (A) Kinetics of melittin adsorption on POPC/chol 70:30 vesicles, as observed by the change of fluorescence intensity at 380 nm, as a function of time, λ_{exc}=280 nm. (Ri=90; [lipid]=3 mM; [melittin]=35 μM). (a) Free melittin, (b) melittin with POPC/chol vesicles. (B) Residual of the simulation of the trace presented in (b) with a mono-exponential function.

2.2. Fluorescence quenching

We have exploited the well-established ability of bromine atoms to quench the tryptophan fluorescence [38–40,49] in order to examine the penetration kinetics of melittin in various lipid matrices. The brominated 6,7Br_2PC was selected because its structure is analogous to that of POPC. As an illustration of the fluorescence quenching caused by 6,7Br_2PC, Fig. 4 displays the fluorescence spectra of melittin/POPC with and without 15 (mol)% Br_2PC. The intensity of the fluorescence is decreased while the profile of the band remains practically the same. The presence of bromine atoms at positions 6–7 leads to a decrease in fluorescence by about 26% (integrated between 300 and 430 nm). A similar behavior is observed for the vesicles formed with POPC/POPG (97:3) for which the quenching is about 33% for the 6–7Br_2PC. In the same conditions, the quenching level for the vesicles containing 30 (mol)% chol is only 10%. These levels of quenching are in agreement with a previous study on small unilamellar vesicles (SUV) prepared with PC, and phosphatidylserine (PS) [26].

In order to probe the quenching associated to the penetration of ^{19}Trp in the hydrophobic core of the bilayer, we have measured the fluorescence intensity at an isoemissive wavelength. As can be shown in Fig. 1, the fluorescence spectra of free and POPC-bound melittin cross at 351 nm. This wavelength is referred to as isoemissive because the intensity of fluorescence at this wavelength does not vary upon the binding of the peptide to the lipid membranes. Therefore, variations in fluorescence intensity at the isoemissive wavelength are directly associated to the

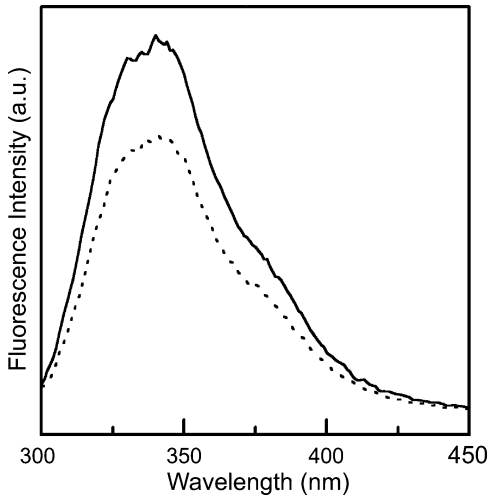

Fig. 4. Fluorescence spectra of melittin in the presence of POPC bilayers: (—) pure POPC; (- - - -) POPC containing 15 mol% 6,7Br_2PC, (Ri=90; [phospholipid]=3 mM; [melittin]=35 μM) (λ_{exc}=280 nm).

quenching. Using the equilibrium spectra obtained for free and bound melittin, we have defined an isoemissive point for each system. Fig. 5 shows the kinetics of insertion of melittin in POPC vesicles, as probed by the variation of the fluorescence intensity at 351 nm. As a control, the upper trace, which displays a fluorescence intensity practically constant, is obtained from the binding of melittin to POPC vesicles, and confirms the choice of the isoemissive point for this system. A similar control was performed for every investigated system. The kinetics trace for melittin binding to Br_2PC-containing vesicles was fitted with a bi-exponential, and the results are presented in Table 2. The role played by negatively charged POPG (3 mol% in POPC) on melittin insertion was probed with the brominated lipid. The decays in fluorescence intensity were also fitted with bi-exponential functions and the resulting parameters are included in Table 2. The kinetics of penetration is faster in the case of the POPG-containing vesicles than for pure POPC vesicles, as illustrated by the larger k_1 value. Conversely, the k_2 value is not significantly different for POPC and POPC/POPG systems. The pre-exponential factor A_1 seems to be slightly affected by the variations happening during the dead time of the set-up as the sum of A_1+A_2+F is less for the POPG-

Table 2
Parameters related to the quenching of the ^{19}Trp fluorescence during the association of melittin with lipid membranes

Parameters	(POPC/6,7Br_2PC)/ melittin	(POPC/6,7Br_2PC/ POPG)/melittin	(POPC/ 6,7Br_2PC/chol)/ melittin
A_1[a]	0.155±0.008	0.138±0.008	0.084±0.007
k_1 (s^{-1})	29±2	38±3	35±4
A_2[a]	0.083±0.008	0.085±0.008	–
k_2 (s^{-1})	1.1±0.1	1.2±0.1	–
F[a]	1.174±0.002	1.090±0.008	1.445±0.007

The lipid composition is indicated at the top of each column and the Ri was 90.
[a] Volt.

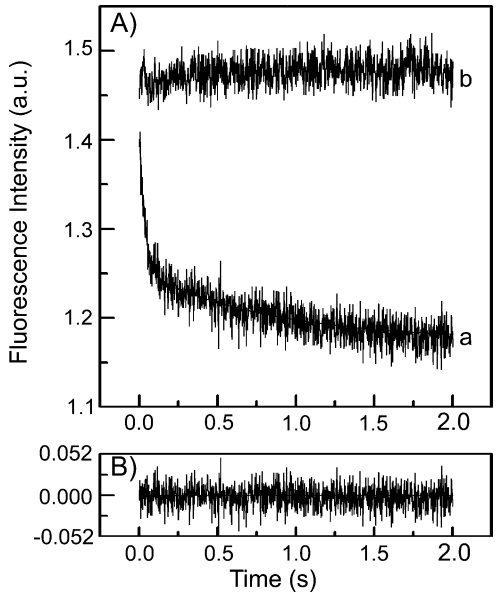

Fig. 5. (A) (a) Quenching of melittin fluorescence, at the isoemissive wavelength (λ=351 nm), upon its binding to POPC bilayers containing 15 mol% 6,7Br_2PC (Ri=90; [phospholipid]=3 mM; [melittin]=35 μM). (b) Variation of the signal measured upon binding to POPC vesicles free of brominated lipids (control experiment). (B) Residual of the simulation of the trace presented in (a) with a bi-exponential function.

containing vesicles. The kinetics of melittin insertion was also examined for the POPC/6,7Br_2PC/chol system. In this case, the decrease of the fluorescence intensity could be simulated using a single exponential; the values determined from the fits are included in Table 2.

2.3. CD measurements

CD measurements were performed to probe the folding of melittin upon binding. Before the addition of vesicles,

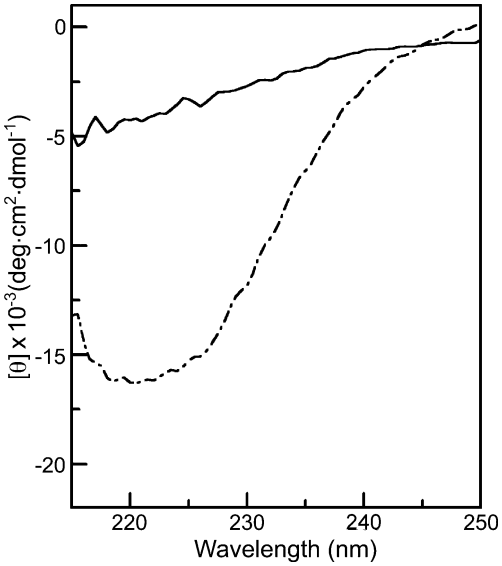

Fig. 6. CD spectra of melittin (—) free in solution, and (- - - -) bound to POPC (Ri=90; [POPC]=3 mM; [melittin]=35 μM).

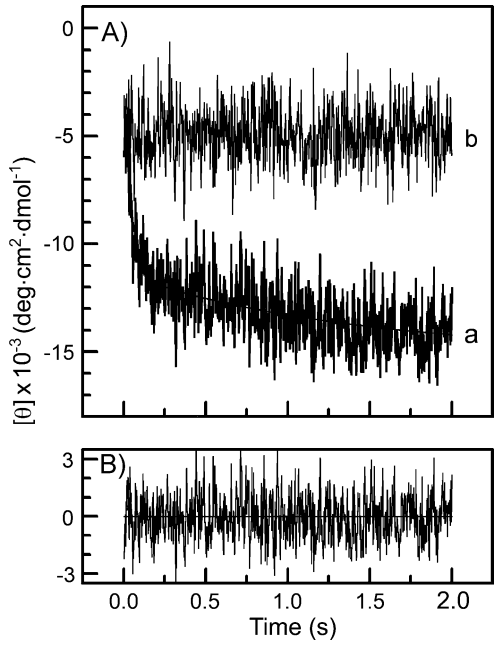

Fig. 7. (A) (a) Kinetics of the helix formation upon melittin binding to POPC vesicles (Ri=90; [POPC]=3 mM; [melittin]=35 μM). The ellipticity was measured at 222 nm. (b) Variation of the signal measured upon the dilution of melittin free in solution (control experiment). (B) Residual of the simulation of the trace presented in (a) with a bi-exponential function.

melittin concentration was sufficiently low that the peptide existed in the monomeric and mainly disordered state [50,51]. In the presence of vesicles, melittin adopts mainly a helical structure [19]. This change of secondary structure upon binding can be followed in a straightforward manner by the CD spectra (Fig. 6). In the absence of vesicle, no distinct feature are observed on the CD spectra, whereas a minimum at 222 nm, characteristic of α-helix, is detected once the peptide is bound to the membranes. The molar ellipticity is about −4000 deg cm^2/dmol for free melittin, in agreement with previous reports [52,53]. This corresponds to a helical content of about 14%. In the presence of vesicles, the molar ellipticity at 222 nm reaches −18,000 deg cm^2/dmol, as previously reported [19,52–54]; this is representative of a α-helix content of about 55%. In the case of the cholesterol-containing vesicles, the molar ellipticity values are considerably smaller (−8000 deg cm^2/dmol); it is associated with incomplete melittin binding, as also inferred from the hypsochromic shift of the ^{19}Trp fluorescence.

The ellipticity at 222 nm was selected to examine the evolution of the secondary structure of melittin upon binding. Fig. 7 shows the kinetics of melittin folding in the presence of POPC vesicles. The control, in the absence of vesicles, indeed shows a horizontal line. The variation of the ellipticity at 222 nm was simulated by a bi-exponential and the resulting parameters are presented in Table 3. The kinetics was also examined for POPC/POPG (97:3) vesicles and the fitted parameters are included in Table 3. The first rate constant, k_1, corresponds to 20 and 23 s^{-1} for POPC and POPC/POPG (97:3) vesicles, respectively. The phenomenon described by the first exponential is the main contribution for the helical folding since A_1 is twice as large as A_2. The F values are similar to those obtained at equilibrium indicating that the kinetics was completely recorded. The kinetics has also been examined for the POPC vesicles in the presence of cholesterol. In this case, a mono-exponential was fitted and the parameters are shown in Table 3. These results show a k_1 value similar to that observed with POPC LUV and, as observed at equilibrium, the magnitude of the molar ellipticity at 222 nm is more limited (about 30% of the change obtained for POPC vesicles).

3. Discussion

The association of melittin with POPC bilayers has been examined using three complementary approaches that allow us to examine the kinetics of the different events happening during the adsorption—the results are summarized in Table 4. First, the change of polarity of ^{19}Trp has been probed with the fluorescence intensity at 380 nm. This change is associated to the fluorescence band shift observed when the Trp residue is transferred from an aqueous environment to an apolar milieu upon melittin binding to membranes [7,36,37]. Second, ^{19}Trp fluorescence quenching by brominated lipids was used to determine the penetration of this residue in the bilayer.

Table 3
Parameters related to the change in ellipticity during the association of melittin with lipid membranes

Parameters	Melittin/POPC[a]	Melittin/[POPC/POPG, (97:3)][a]	Melittin/[POPC/POPG, (97:3)][b]	Melittin/[POPC/chol (70:30)]
A_1[c]	8.0±0.5	7.0±0.6	9.5±0.6	3.1±0.5
k_1 (s^{-1})	20±2	23±3	25±3	28±5
A_2[c]	3.7±0.5	4.2±0.6	3.8±0.3	–
k_2 (s^{-1})	0.7±0.2	1.5±0.2	1.8±0.3	–
F[c]	−15.1±0.5	−18.4±0.6	−18.1±0.1	−7.2±0.5

The lipid composition is indicated at the top of each column and the Ri was 90.
[a] Buffer containing 10 mM NaCl.
[b] Buffer containing 20 mM NaCl.
[c] deg cm^2 dmol^{-1}.

Table 4
Summary of the kinetics parameters for the association of melittin with POPC bilayers (Ri 90)

Parameters	^{19}Trp Polarity	^{19}Trp-fluorescence quenching with 6,7Br$_2$PC	Circular dichroism
A_1[a]	0.33±0.01	0.155±0.008	8.0±0.5
k_1(s^{-1})	32±2 (29–37)	29±2 (24–34)	20±2 (16–27)
τ_1(ms)[b]	31±2 (27–35)[c]	35±3 (29–42)	50±5 (39–63)
A_2[a]	0.34±0.01	0.083±0.008	3.7±0.5
k_2 (s^{-1})	2.6±0.1 (2.4–2.7)	1.1±0.1 (0.8–1.4)	0.7±0.2 (0.17–1.2)
τ_2(ms)[b]	386±15 (370–410)	922±64 (730–1300)	1430±330 (790–6000)
F	1.57±0.01	1.174±0.008	−15.1±0.5

[a] Volt or deg · cm^2 · dmol^{-1}.
[b] $\tau=1/k$.
[c] The values in parentheses represent the end points of the 67% confidence interval determined by the support plane procedure [71].

The brominated lipids were selected because they are miscible with POPC and the small size of bromine atoms has been shown to cause very limited perturbations in bilayers. In fact, bilayers prepared with 6,7Br$_2$PC have almost the same thickness as those formed with pure POPC [55]. Moreover, we introduced a limited proportion of brominated lipids (15 mol%) in the systems, providing a reliable comparison of the results obtained by the three different approaches. The average position of the bromine atoms in the bilayers has been determined by X-ray diffraction [55]. The average distance of 6,7Br$_2$PC relative to the middle of the bilayer is 11 Å. This location is indeed not fixed in space and time for fluid bilayers. The position distribution of the bromine atoms has been associated to a Gaussian distribution with a half-height width of 4 Å [39,55]. The quenching process likely results from a heavy atom-induced perturbation of spin-orbital coupling [56]. For 6,7Br$_2$PC-containing POPC bilayers, we measured a quenching of 26% of the fluorescence of the adsorbed melittin. This equilibrium value is consistent with those previously reported [26] and with the fact that the ^{19}Trp of melittin penetrates at least in the glycerol backbone area [36,39,53,57]. Third, the CD spectra are consistent with the well-established transition experienced by melittin upon membrane binding, from a random coil to a helical structure [19,52,53].

For the adsorption of melittin on POPC vesicles, all the kinetics curves showed two components. Few hypotheses can be at the origin of these. First, two distinct populations of melittin molecules could co-exist and bind at different rates. This should be specifically considered in the case of melittin since previous reports have shown that monomers and tetramers could be obtained in solution. However, the CD results suggest that this hypothesis can be rejected since the initial molar ellipticity is typical of the monomer [35,52–54]. Moreover, the presence of isoemissive points supports the presence of only two states; one free and one bound state. It was also argues that bound melittin molecules embedded in membranes are dispersed instead of aggregated [58,59]. Therefore, the two exponentials are most likely associated to two sequential events occurring during melittin adsorption. The bi-exponential functions are descriptive of two sequential and irreversible events [48]. It has been shown that melittin association to membranes is practically irreversible [6] and, more recently, a SPR study concluded that the melittin association to bilayers was considerably faster than its dissociation [34]. Therefore, at this point, the rates for the dissociation are neglected. The rate constants are in the order of 30 and 1 s^{-1}. These changes occur prior to melittin translocation across the membrane since it has been shown to be much slower, in the order of minutes [5]. The two events, both leading to a less polar environment of the tryptophan, and a closer contact with the bromine atoms on the acyl chains, suggest that the association of melittin is a two-step process: the first step would be the adsorption of the peptide at the lipid–water, followed by a deeper insertion of the peptide in the membrane, leading to additional ^{19}Trp-fluorescence quenching and a more apolar environment for this residue.

In the case of the first exponential, the results obtained on the three different lipid systems share the same feature: the rate constants are close with one another suggesting that insertion and folding are strongly coupled. When penetrating in the apolar core of the membrane, the peptide can maintain the H-bonds involving its amide groups previously satisfied with water molecules, by structuring itself in a helix to create intramolecular H-bonds [19]. In fact, it was shown previously, using melittin diastereoisomers, that the folding as a α-helix favors, from a thermodynamics point of view, the partitioning of the peptide in POPC bilayers [19]. Our results, consistent with this view, provide a novel kinetics aspect related to the association. For the three investigated systems, the kinetics results indicate that the folding as a α-helix undergoes at a slightly slower rate than the sensing of ^{19}Trp of a less polar environment. This finding indicates that melittin binds as a disordered monomeric peptide, inserts in the lipid membrane, and its concerted folding in helix is promoted by the peptide penetration. In other words, from the kinetics point of view, the folding is a consequence of the insertion. Interestingly, a similar sequence (i.e. a change in polarity, indicative of peptide adsorption, with a slightly faster rate than that of the formation of helix) has also been observed for the main sequence of the sub-unit IV of cytochrome *c* oxidase [60]. This behavior may be a general trend in membrane peptide folding.

The second event, associated with the second exponential, also leads to a less polar environment of the ^{19}Trp, an increased quenching of the fluorescence of this residue, and an increase in helix content. It is proposed that this event corresponds to a deeper insertion in the lipid bilayer. The characteristic times associated with the second event are considerably slower than for the first one (between 12 and 38 times longer). During this second step, the change in

polarity appears to be again the fastest event. This second step is significant in the partitioning process because the pre-exponential factors indicate that its contribution is about 30–50% of the total changes. In the case of two sequential and irreversible events, the pre-exponential factors are directly related to the relative contributions of the phenomena described by the exponentials when k_1 is much larger than k_2 [48], and this condition is reasonably met in our case. The pre-exponential factors of the kinetics obtained from the hypsochromic shift can have many interpretations because there is no linear relationship between the magnitude of the shift and the depth of penetration. Similarly, the fluorescence quenching does not show a simple behavior as a function of depth penetration [40]. However, the change in helical content is more straightforward to interpret and our results indicate that about 65% of the final helical content is formed during the first step. It is known that ^{14}Pro of melittin leads to a kink in the helix [18], and the two helix segments are proposed to adopt different orientations in lipid membranes [18,61]. It is possible that ^{14}Pro also breaks the kinetics of melittin adsorption into two, the two helical segments being inserted and formed with their own characteristic times. It has been inferred from another set of kinetics measurements [33] that the helical segment near the N-terminus makes the first contact with the bilayer. Since this segment includes about 65% of the helix content, our results are supportive of this proposed mechanism.

There are few studies in the literature reporting the kinetics of melittin binding to phosphocholine bilayers in the millisecond range [31–33,51]. Our series of measurements on PC membranes is in good agreement with those previously obtained by probing melittin adsorption at the interface from the changes of the surface potential induced by the charged residues [33]. In that study, the kinetics of adsorption was simulated by a bi-exponential with rate constants of 27 ± 11 s^{-1}, and 3.70 ± 0.04 s^{-1}. The reported values, representing the adsorption of the charged residues (mainly located at the C-terminal, ^{21}Lys-^{22}Arg-^{23}Lys-^{24}Arg), are comparable to those that are reported here for ^{19}Trp. This agreement should be expected considering the physical proximity of the probed residues. That paper also reports the kinetics of the quenching of the ^{19}Trp fluorescence upon melittin binding to bilayers containing brominated PC, for a Ri of 45. The fluorescence decrease was fitted with a bi-exponential but the rate constants (k_1=112±16 s^{-1} and k_2=11.0±0.3 s^{-1}) were significantly larger than those measured here. This difference is surprising taking into account the good consistency between our quenching results and their results obtained from the surface charge. In addition, it is somehow difficult to reconcile such different kinetics for neighbouring segments. The use of tetrabrominated lipids, and the filter approach used to measure the fluorescence intensity may be at the origin of this discrepancy. The temperature and the type of PC are not indicated in that previous report and some potential differences could also explain the differences. The other measurements of the association kinetics of melittin with lipid bilayers were performed with SUV made of dimyristoyl-*sn*-glycero-3-phosphocholine (DMPC), dipalmitoyl-*sn*-glycero-3-phosphocholine (DPPC) or dioleoyl-*sn*-glycero-3-phosphocholine (DOPC) [31,32,51]. In all these cases, the kinetics showed a single exponential. For the three PC investigated in similar experimental conditions (similar Ri, and lipids in the liquid crystalline phase), the resulting k values were 37±4, 23±7, and 91 s^{-1} for DMPC, DPPC [32], and DOPC [51], respectively. The results obtained with saturated lipids are similar to those reported here for the first exponential with POPC. The kinetics with DOPC is three times faster, a difference that was proposed to be associated with the higher degree of chain unsaturation [31]. The absence of the second contribution may be associated to the use of SUV. It is known that SUV bilayers are under tension [62] and this aspect can influence the insertion mechanism. It has been reported for example, that melittin binding was enhanced for SUV compared to LUV [30], a phenomenon that was associated to the difference in lipid packing and membrane defects. Clearly, these could also affect the adsorption kinetics. It must be pointed out though that the extruded LUV used in this study had a diameter of about 50 nm; this relatively small diameter may have an influence on the kinetics of association (for example, even though lipid bilayers are a soft material, it could be more difficult for melittin to lie flat on this curved surface). It is however interesting to observe that the agreement in the number of exponentials required to reproduce the kinetics appears, at this point, to be associated with the method of preparation of the unilamellar vesicles.

For the POPG-containing membranes, the hypsochromic shift of the ^{19}Trp fluorescence is about 16–17 nm, a shift that is slightly more pronounced than that observed the zwitterionic POPC bilayers. This observation is consistent with the variation of the ^{19}Trp environment observed previously in the presence of negatively charged lipids [12]. It must be noted that, at Ri=90, melittin is practically completely bound in the case of POPC and POPC/POPG bilayers, and as a consequence, the observed differences cannot be attributed to different proportions of bound melittin. The quenching was also more pronounced in the presence of POPG. This observation is in agreement with previous results reporting a deeper penetration of ^{19}Trp of melittin in cardiolipin bilayers compared to PC ones [63]. It was also proposed that the association of melittin with negatively charged membranes leads to a more limited penetration of the water molecules in the regions neighbouring ^{19}Trp than in the case of zwitterionic membranes [12]. This effect could also explain the fluorescence shift and increased quenching that were observed here. The CD results indicate that melittin displays a similar helix structure once bound to POPC/POPG (97:3) and POPC bilayers, in agreement with the previous studies [12,19].

Table 5
Summary of the kinetics parameters for the association of melittin with POPC/POPG (97:3) bilayers (Ri 90)

Parameters	^{19}Trp polarity	^{19}Trp-fluorescence quenching with 6,7Br$_2$PC	Circular dichroism
A_1[a]	0.33±0.01	0.138±0.008	7.0±0.6
k_1 (s^{-1})	48±3 (42–56)	38±3 (30–45)	23±3 (16–31)
τ_1 (ms)[b]	21±1 (18–24)[c]	26±2 (22–33)	44±6 (32–61)
A_2[a]	0.29±0.01	0.085±0.008	4.2±0.6
k_2 (s^{-1})	2.30±0.05 (2.2±2.4)	1.2±0.1 (1.0±1.4)	1.5±0.2 (0.9±2.0)
τ_2 (ms)[b]	435±9 (410±450)	814±60 (690±1000)	667±80 (500±1100)
F	1.49±0.01	1.090±0.008	−18.4±0.6

[a] Volt or deg · cm^2 · $dmol^{-1}$.
[b] $\tau=1/k$.
[c] The values in parenthesis represent the end points of the 67% confidence interval determined by the support plane procedure [71].

The features of the kinetics of melittin adsorption to POPG-containing bilayers are the same as those obtained with pure POPC membranes—the results are summarized in Table 5. First, the kinetics curves obtained by the three techniques show bi-exponential shapes. Second, the three rate constants associated with the first step are similar, suggesting coupled events. Third, for this first step, the rate constant associated to the change of ^{19}Trp environment is greater than that associated with the peptide folding. Our results also reveal that the characteristic times of the first exponential are shorter in the presence of negatively charged lipids compared to those measured on pure POPC bilayers; this influence is observed for POPG proportions as small as 3 mol% and is dependent on the POPG proportion. The faster association of melittin to negatively charged membranes as observed by the ^{19}Trp-fluorescence shift was reported with systems including PS. The introduction of 15 mol% PS in PC led to a bi-exponential kinetics with rate constants similar to those reported here [33] while with pure DMPS bilayers, the ^{19}Trp-fluorescence shift happened completely during the dead time of the spectrometer (3 ms) [31]. We conclude that the attractive electrostatic interactions between the peptide and negatively charged membranes act early in the binding process as they are long-distance interactions. It has been proposed that membrane lipids could play a role in membrane protein folding [28]. It was shown for example, that the bending rigidity of bilayers affects bacteriorhodopsin folding [64]. The results presented here indicate that the surface charge density of membranes can also be a factor modulating peptide/protein insertion in membranes.

In our experiments with POPC/chol system, melittin is not completely bound, in agreement with the reported reduced affinity of melittin for these membranes [7,8]. As a result, the hypsochromic shift is less pronounced, the quenching by the brominated lipids is less efficient, and the overall helix proportion is reduced compared to the results obtained with POPC vesicles. In our conditions, it is estimated, on the basis of the shift of the ^{19}Trp fluorescence and of its quenching, that about 40% of melittin is associated with POPC/chol membranes. Higher LUV concentrations could not be used without introducing a significant light diffusion contribution that was practically impossible to correct properly. It was previously proposed that melittin insertion was limited in cholesterol-containing membranes [8,16,65]. It is well established that phosphatidylcholine membranes containing 30 (mol)% chol exist in the liquid ordered phase [13–15], and the tight lipid packing combined with the highly ordered lipid acyl chains are unfavorable to the association of melittin—a phenomenon observed with other peptides including mastoporan [66], and nisin [67]. The kinetics data for this system are summarized in Table 6. As for the two other investigated systems, the rate constants associated to the three measurements are close with one another, and the shortest characteristic time is associated to the change in Trp environment. These two features do not appear to be sensitive to the nature of the lipid bilayers. Our kinetics measurements also reveal the mono-exponential behavior of the association kinetics of melittin with cholesterol-containing membranes. The rate constants obtained from these measurements are in the range obtained for the short-time component of the bi-exponential kinetics obtained with POPC, and POPC/POPG LUVs. This observation is consistent with the hypothesis that the second component corresponds to a deeper penetration of melittin in the apolar core of the bilayer and that the liquid ordered phase induced by the presence of cholesterol prevents this deeper penetration of the peptide in the lipid membranes. Alternatively, it is also possible that there is not enough melittin bound to the surface of the vesicles to allow a deeper penetration as this step could be a cooperative event.

In conclusion, the results presented here may provide some insights into membrane protein folding. It is inferred that, from a kinetics point of view, folding is a consequence of the initial insertion of melittin in lipid membranes. It is established that, during the folding of soluble peptides/proteins from the unfolded state, elements of the secondary structures, such as helices, are formed within 5–10 ms (for a review, see Ref. [68]). Moreover, protein folding has been

Table 6
Summary of the kinetics parameters for the association of melittin with POPC/chol bilayers (Ri 90)

Parameters	^{19}Trp Polarity	^{19}Trp-fluorescence quenching with 6,7Br$_2$PC	Circular dichroism
A[a]	0.23±0.01	0.084±0.007	3.1±0.5
k_1 (s^{-1})	40±3 (34–43)	35±4 (28–42)	28±5 (21–38)
τ (ms)[b]	25±1 (23–29)[c]	29±3 (24–36)	35±6 (26–48)
F	2.06±0.01	1.445±0.007	−7.2±0.5

[a] Volt or deg · cm^2 · $dmol^{-1}$.
[b] $\tau=1/k$.
[c] The values in parenthesis represent the end points of the 67% confidence interval determined by the support plane procedure [71].

observed with sub-millisecond rates and the formation of helices has been estimated to take place within ≈100 ns [69]. The rate constant for the folding of membrane-bound melittin appears, in comparison, to be rather slow. However, this could be a consequence of the rate of the peptide insertion (i.e. the rate of the drastic reduction in dielectric constant and hydrogen bonding capabilities of the surrounding), which would trigger the folding. The slow formation of a helical segment in bacteriorhodopsin has been reported (apparent rate in the order of 0.01 s^{-1}), and was found to be a rate-limiting step in the protein folding [70]. The authors suggested, as one possible explanation, that this slow folding could be associated with a slow insertion of the sequence in the membrane. In addition, that study proposed that some bilayer properties (namely the bending rigidity) could modulate the kinetics of the folding. It is proposed [28] that the rate-limiting folding step might be directly associated to the rate-limiting insertion of helices in the case of bacteriorhodopsin. The rate of melittin folding was found to be influenced by the lipid composition of the bilayer and we propose that this was achieved by the modulation of the kinetics of insertion. We believe that this relatively simple system provides a clear example of coupled penetration and folding. This additional level of complexity in membrane protein folding must be examined in detail.

Acknowledgements

The authors thank the Natural Sciences and Engineering Research Council of Canada, and the Fonds FCAR (Québec) for their financial support. They also thank Prof. Jeffrey Keillor (Department of Chemistry, Université de Montréal) for providing access to his stop-flow spectrometer.

References

[1] E. Habermann, Bee and wasp venoms, Science 177 (1972) 314–322.
[2] C.E. Dempsey, The actions of melittin on membranes, Biochim. Biophys. Acta 1031 (1990) 143–161.
[3] W.F. DeGrado, G.F. Musso, M. Lieber, E.T. Kaiser, F.J. Kézdy, Kinetics and mechanism of hemolysis induced by melittin and by a synthetic melittin analogue, Biophys. J. 37 (1982) 329–338.
[4] M.T. Tosteson, S.J. Holmes, M. Razin, D.C. Tosteson, Melittin lysis of red cells, J. Membr. Biol. 87 (1985) 35–44.
[5] K. Matsuzaki, S. Yoneyama, K. Miyajima, Pore formation and translocation of melittin, Biophys. J. 73 (1997) 831–838.
[6] T. Benachir, M. Lafleur, Study of vesicle leakage induced by melittin, Biochim. Biophys. Acta 1235 (1995) 452–460.
[7] T. Benachir, M. Monette, J. Grenier, M. Lafleur, Melittin-induced leakage from phosphatidylcholine vesicles is modulated by cholesterol: a property used for membrane targeting, Eur. Biophys. J. 25 (1997) 201–210.
[8] D. Allende, T.J. McIntosh, Lipopolysaccharides in bacterial membranes act like cholesterol in eukaryotic plasma membranes in providing protection against melittin-induced bilayer lysis, Biochemistry 42 (2003) 1101–1108.
[9] S. Ohki, E. Marcus, D.K. Sukumaran, K. Arnold, Interaction of melittin with lipid membranes, Biochim. Biophys. Acta 1194 (1994) 223–232.
[10] M.J. Gómara, S. Nir, J.L. Nieva, Effects of sphingomyelin on melittin pore formation, Biochim. Biophys. Acta 1612 (2003) 83–89.
[11] S.H. Portlock, M.J. Clague, R.J. Cherry, Leakage of internal markers from erythrocytes and lipid vesicles induced by melittin, gramicidin S and alamethicin: a comparative study, Biochim. Biophys. Acta 1030 (1990) 1–10.
[12] A.K. Ghosh, R. Rukmini, A. Chattopadhyay, Modulation of tryptophan environment in membrane-bound melittin by negatively charged phospholipids: implications in membrane organization and function, Biochemistry 36 (1997) 14291–14305.
[13] M.R. Vist, J.H. Davis, Phase equilibria of cholesterol/dipalmitoylphosphatidylcholine mixtures: ^{2}H nuclear magnetic resonance and differential scanning calorimetry, Biochemistry 29 (1990) 451–464.
[14] J.L. Thewalt, M. Bloom, Phosphatidylcholine: cholesterol phase diagrams, Biophys. J. 63 (1992) 1176–1181.
[15] T.P.W. McMullen, R.N.A.H. Lewis, R.N. McElhaney, Calorimetric and spectroscopic studies of the effects of cholesterol on the thermotropic phase behavior and organization of a homologous series of linear saturated phosphatidylethanolamine bilayers, Biochim. Biophys. Acta 1416 (1999) 119–134.
[16] D. Allende, A. Vidal, S.A. Simon, T.J. McIntosh, Bilayer interfacial properties modulate the binding of amphipathic peptides, Chem. Phys. Lipids 122 (2003) 65–76.
[17] A.S. Ladokhin, S.H. White, 'Detergent-like' permeabilization of anionic lipid vesicles by melittin, Biochim. Biophys. Acta 1514 (2001) 253–260.
[18] T.C. Terwilliger, L. Weissman, D. Eisenberg, The structure of melittin in the form I crystals and its implication for melittin's lytic and surface activities, Biophys. J. 37 (1982) 353–361.
[19] A.S. Ladokhin, S.H. White, Folding of amphipathic α-helices on membranes: energetics of helix formation by melittin, J. Mol. Biol. 285 (1999) 1363–1369.
[20] D. Eisenberg, R.M. Weiss, T.C. Terwilliger, The helical hydrophobic moment: a measure of the amphiphilicity of a helix, Nature 299 (1982) 371–374.
[21] L.M. Gierasch, Signal sequences, Biochemistry 28 (1989) 923–930.
[22] R.M. Epand, S.-W. Hui, C. Argan, L.L. Gillespie, G.C. Shore, Structural analysis and amphiphilic properties of a chemically synthesized mitochondrial signal peptide, J. Biol. Chem. 261 (1986) 10017–10020.
[23] C.L. Bashford, G.M. Alder, G. Menestrina, K.J. Micklem, J.J. Murphy, C.A. Pasternak, Membrane damage by hemolytic viruses, toxins, complement, and other cytotoxic agents. A common mechanism blocked by divalent cations, J. Biol. Chem. 261 (1986) 9300–9308.
[24] R.O. Laine, B.P. Morgan, A.F. Esser, Comparison between complement and melittin hemolysis: anti-melittin antibodies inhibit complement lysis, Biochemistry 27 (1988) 5308–5314.
[25] A. Baghian, J. Jaynes, F. Enright, K.G. Kousoulas, An amphipathic α-helical synthetic peptide analogue of melittin inhibits herpes simplex virus-1 (HSV-1)-induced cell fusion and virus spread, Peptides 18 (1997) 177–183.
[26] Z. Oren, Y. Shai, Selective lysis of bacteria but not mammalian cells by diastereomers of melittin: structure–function study, Biochemistry 36 (1997) 1826–1835.
[27] M.E. Houston Jr., L.H. Kondejewski, D.N. Karunaratne, M. Gough, S. Fidai, R.S. Hodges, R.E.W. Hancock, Influence of preformed α-helix and α-helix induction on the activity of cationic antimicrobial peptides, J. Pept. Res. 52 (1998) 81–88.
[28] P.J. Booth, A.R. Curran, Membrane protein folding, Curr. Opin. Struct. Biol. 9 (1999) 115–121.
[29] G. Schwarz, R. Zong, T. Popescu, Kinetics of melittin induced pore formation in the membrane of lipid vesicles, Biochim. Biophys. Acta 1110 (1992) 97–104.

[30] S. Rex, G. Schwarz, Quantitative studies on the melittin-induced leakage mechanism of lipid vesicles, Biochemistry 37 (1998) 2336–2345.
[31] K.M. Sekharam, T.D. Badrick, S. Georghiou, Kinetics of melittin binding to phospholipid small unilamellar vesicles, Biochim. Biophys. Acta 1063 (1991) 171–174.
[32] T.D. Badrick, A. Philippetis, S. Georghiou, Stopped-flow fluorometric study of the interaction of melittin with phospholipid bilayers: importance of the physical state of the bilayer and the acyl chain length, Biophys. J. 69 (1995) 1999–2010.
[33] C. Wolfe, J. Cladera, P. O'Shea, Amino acid sequences which promote and prevent the binding and membrane insertion of surface-active peptide: comparison of melittin and promelittin, Mol. Membr. Biol. 15 (1998) 221–227.
[34] N. Papo, Y. Shai, Exploring peptide membrane interaction using surface plasmon resonance: differentiation between pore formation versus membrane disruption by lytic peptides, Biochemistry 42 (2003) 458–466.
[35] J.C. Talbot, J. Dufourcq, J. DeBony, J.F. Faucon, C. Lussan, Conformational change and self association of monomeric melittin, FEBS Lett. 102 (1979) 191–193.
[36] A.M. Batenburg, J.C.L. Hibbeln, B. de Kruijff, Lipid specific penetration of melittin into phospholipid model membranes, Biochim. Biophys. Acta 903 (1987) 155–165.
[37] J. Dufourcq, J.-F. Faucon, Intrinsic fluorescence study of lipid–protein interactions in membrane models. Binding of melittin, an amphipathic peptide, to phospholipid vesicles, Biochim. Biophys. Acta 467 (1977) 1–11.
[38] T. Markello, A. Zlotnick, J. Everett, J. Tennyson, P.W. Holloway, Determination of topography of cytochrome b_5 in lipid vesicles by fluorescence quenching, Biochemistry 24 (1985) 2895–2901.
[39] A.S. Ladokhin, Distribution analysis of depth-dependent fluorescence quenching in membranes: a practical guide, Methods Enzymol. 278 (1997) 462–473.
[40] E.J. Bolen, P.W. Holloway, Quenching of tryptophan fluorescence by brominated phospholipid, Biochemistry 29 (1990) 9638–9643.
[41] H. Vogel, F. Jähnig, The structure of melittin in membranes, Biophys. J. 50 (1986) 573–582.
[42] S. Rex, J. Bian, J.R. Silvius, M. Lafleur, The presence of PEG-lipids in liposomes does not reduce melittin binding but decreases melittin-induced leakage, Biochim. Biophys. Acta 1558 (2002) 211–221.
[43] C.H. Fiske, Y. Subbarow, The colorimetric determination of phosphorus, J. Biol. Chem. 66 (1925) 375–400.
[44] J. Dufourcq, J.-F. Faucon, G. Fourche, J.-L. Dasseux, M. Le Maire, T. Gulik-Krzywicki, Morphological changes of phosphatidylcholine bilayers induced by melittin: vesicularization, fusion, discoidal particles, Biochim. Biophys. Acta 859 (1986) 33–48.
[45] A.S. Ladokhin, S. Jayasinghe, S.H. White, How to measure and analyze tryptophan florescence in membranes properly, and why bother? Anal. Biochem. 285 (2000) 235–245.
[46] C.A. Rohl, R.L. Baldwin, Comparison of NH exchange and circular dichroism as techniques for measuring the parameters of the helix–coil transition in peptides, Biochemistry 36 (1997) 8435–8442.
[47] A.M. Batenburg, J.H. van Esch, J. Leunissen-Bijvelt, A.J. Verkleij, B. de Kruijff, Interaction of melittin with negatively charged phospholipids: consequences for lipid organisation, FEBS Lett. 223 (1987) 148–154.
[48] J.H Espenson, Chemical Kinetics and Reaction Mechanisms, McGraw-Hill Book, 1981.
[49] W.C. Wimley, S.H. White, Determining the membrane topology of peptides by fluorescence quenching, Biochemistry 39 (2000) 161–170.
[50] J.F. Faucon, J. Dufourcq, C. Lussan, The self-association of melittin and its binding to lipids—an intrinsic fluorescence polarization study, FEBS Lett. 102 (1979) 187–190.
[51] G. Schwartz, G. Beschiaschvili, Thermodynamic and kinetic studies on the association of melittin with a phospholipid bilayer, Biochim. Biophys. Acta 979 (1989) 82–90.
[52] Y. Hagihara, M. Kataoka, S. Aimoto, Y. Goto, Charge repulsion in the conformational stability of melittin, Biochemistry 31 (1992) 11908–11914.
[53] H. Vogel, Incorporation of melittin into phosphatidylcholine bilayers, FEBS Lett. 134 (1981) 37–42.
[54] A.F. Drake, R.C. Hider, The structure of melittin in lipid bilayer membranes, Biochim. Biophys. Acta 555 (1979) 371–373.
[55] T.J. McIntosh, P.W. Holloway, Determination of depth of bromine atoms in bilayers formed from bromolipid probes, Biochemistry 26 (1987) 1783–1788.
[56] A.S. Ladokhin, Analysis of protein and peptide penetration into membranes by depth-dependent fluorescence quenching: theoretical considerations, Biophys. J. 76 (1999) 946–955.
[57] E. Kuchinka, J. Seelig, Interaction of melittin with phosphatidylcholine membranes. Binding isotherm and lipid head-group conformation, Biochemistry 28 (1989) 4216–4221.
[58] M.-T. Lee, F.-Y. Chen, H.W. Huang, Energetics of pore formation induced by membrane active peptides, Biochemistry 43 (2004) 3590–3599.
[59] F.-Y. Chen, M.-T. Lee, H.W. Huang, Evidence for membrane thinning effect as the mechanism for peptide-induced pore formation, Biophys. J. 84 (2003) 3751–3758.
[60] C. Golding, S. Senior, M.T. Wilson, P. O'Shea, Time resolution of binding and membrane insertion of a mitochondrial signal peptide: correlation with structural changes and evidence for cooperativity, Biochemistry 35 (1996) 10931–10937.
[61] J.W. Brauner, R. Mendelsohn, F.G. Prendergast, Attenuated total reflectance Fourier transform infrared studies of the interaction of melittin, two fragments of melittin, and δ-hemolysin with phosphatidylcholines, Biochemistry 26 (1987) 8151–8158.
[62] B. De Kruijff, P.R. Cullis, G.K. Radda, Differential scanning calorimetry and ^{31}P NMR studies on sonicated and unsonicated phosphatidylcholine liposomes, Biochim. Biophys. Acta 406 (1975) 6–20.
[63] A.M. Batenburg, J.C.L. Hibbeln, A.J. Verkleij, B. De Kruijff, Melittin induces H_{II} phase formation in cardiolipin model membranes, Biochim. Biophys. Acta 903 (1987) 142–154.
[64] P.J. Booth, M.L. Riley, S.L. Flisch, R.H. Templer, A. Farooq, A.R. Curran, N. Chadborn, P. Wright, Evidence that bilayer bending rigidity affects membrane protein folding, Biochemistry 36 (1997) 197–203.
[65] M. Monette, M.-R. Van Calsteren, M. Lafleur, Effect of cholesterol on the polymorphism of dipalmitoylphosphatidylcholine/melittin complexes: an NMR study, Biochim. Biophys. Acta 1149 (1993) 319–328.
[66] T. Katsu, M. Kuroko, T. Morikawa, K. Sanchika, H. Yamanaka, S. Shinoda, Y. Fujita, Interaction of wasp venom mastoporan with biomembranes, Biochim. Biophys. Acta 1027 (1990) 185–190.
[67] R. El Jastimi, K. Edwards, M. Lafleur, Characterization of permeability and morphological perturbations induced by nisin on phosphatidylcholine membranes, Biophys. J. 77 (1999) 842–852.
[68] C.R. Matthews, Pathways of protein folding, Ann. Rev. Biochem. 62 (1993) 653–683.
[69] W.A. Eaton, V. Muńoz, P.A. Thompson, C.-K. Chan, J. Hofrichter, Submillisecond kinetics of protein folding, Curr. Opin. Struct. Biol. 7 (1997) 10–14.
[70] M.L. Riley, B.A. Wallace, S.L. Flitsch, P.J. Booth, Slow α helix formation during folding of a membrane protein, Biochemistry 36 (1997) 192–196.
[71] M.L. Johnson, Multiple-domain fluorescence lifetime data analysis, Methods Enzymol. 278 (1997) 570–583.